Dynamics of actomyosin interactions in relation to the cross-bridge cycle

Wei Zeng[1]**, Paul B. Conibear**[1]**, Jane L. Dickens**[1]**, Ruth A. Cowie**[1]**, Stuart Wakelin**[1]**, András Málnási-Csizmadia**[2] **and Clive R. Bagshaw**[1*]

[1]*Department of Biochemistry, University of Leicester, Leicester LE1 7RH, UK*
[2]*Department of Biochemistry, Eötvös University, H-1117 Budapest, Hungary*

Transient kinetic measurements of the actomyosin ATPase provided the basis of the Lymn–Taylor model for the cross-bridge cycle, which underpins current models of contraction. Following the determination of the structure of the myosin motor domain, it has been possible to introduce probes at defined sites and resolve the steps in more detail. Probes have been introduced in the *Dicytostelium* myosin II motor domain via three routes: (i) single tryptophan residues at strategic locations throughout the motor domain; (ii) green fluorescent protein fusions at the N and C termini; and (iii) labelled cysteine residues engineered across the actin-binding cleft. These studies are interpreted with reference to motor domain crystal structures and suggest that the tryptophan (W501) in the relay loop senses the lever arm position, which is controlled by the switch 2 open-to-closed transition at the active site. Actin has little effect on this process *per se*. A mechanism of product release is proposed in which actin has an indirect effect on the switch 2 and lever arm position to achieve mechanochemical coupling. Switch 1 closing appears to be a key step in the nucleotide-induced actin dissociation, while its opening is required for the subsequent activation of product release. This process has been probed with F239W and F242W substitutions in the switch 1 loop. The E706K mutation in skeletal myosin IIa is associated with a human myopathy. To simulate this disease we investigated the homologous mutation, E683K, in the *Dictyostelium* myosin motor domain.
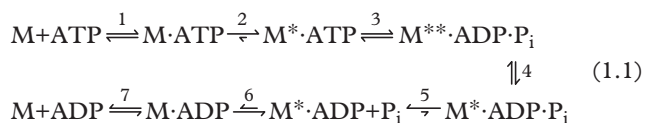
Keywords: myosin; stopped flow; tryptophan; fluorescence; *Dictyostelium*; myopathy

1. INTRODUCTION

The proposal of the sliding filament hypothesis in 1954 challenged the prevailing idea that the contractile proteins themselves underwent large-scale conformational changes to cause shortening of muscle (Huxley & Hanson 1954; Huxley & Niedergerke 1954). Instead, the problem was reformulated in terms of identifying the interactions between the thick and thin filaments that led to their sliding. Subsequently, the cross-bridge, an element of myosin that projected towards the thin filament, was proposed to undergo repetitive interactions with binding sites on the actin subunits to cause net movement (A. F. Huxley 1957; H. E. Huxley 1969). The coupling of this mechanical cycle to the ATPase cycle was clarified by transient kinetics studies of the isolated proteins in solution by Lymn & Taylor (1971). Here, it was shown that ATP binding caused the dissociation of actomyosin before the hydrolysis step and that actin rebound to the myosin–products complex to achieve activation of the ATPase. In the absence of actin, myosin hydrolysed ATP rapidly but the products ADP and P_i remain bound for many seconds. The tight binding of substrate and low turnover number of myosin made this system very favourable for transient kinetic analysis as

intermediates accumulate and decay in succession. Indeed, the tryptophan residues within the myosin provided a natural probe of intermediate states that could be detected by fluorescence (Bagshaw *et al.* 1972). Such measurements showed that ATP binding to myosin was accompanied by a protein isomerization prior to the hydrolysis step, while isomerizations also limited the rate of P_i and ADP release (Bagshaw & Trentham 1974; Bagshaw *et al.* 1974).

Most early biochemical kinetic studies were performed on myosin prepared from rabbit skeletal muscle. Here, the ATP binding isomerization is accompanied by a 10% increase in tryptophan fluorescence (denoted by a single asterisk) while ATP hydrolysis results in a further enhancement in fluorescence to a total of *ca.* 20% (denoted by a double asterisk) relative to the starting apo-state (Johnson & Taylor 1978; Millar & Geeves 1988). The elementary steps in the ATPase mechanism identified by this signal are:

$$M + ATP \underset{1}{\rightleftharpoons} M \cdot ATP \underset{2}{\rightleftharpoons} M^* \cdot ATP \underset{3}{\rightleftharpoons} M^{**} \cdot ADP \cdot P_i$$
$$\updownarrow 4 \qquad (1.1)$$
$$M + ADP \underset{7}{\rightleftharpoons} M \cdot ADP \underset{6}{\rightleftharpoons} M^* \cdot ADP + P_i \underset{5}{\rightleftharpoons} M^* \cdot ADP \cdot P_i$$

By the use of $^{32}P_i$-labelled ATP and ^{18}O exchange measurements, it was demonstrated that the hydrolysis step 3 was freely reversible with an equilibrium constant between 1 and 10, depending on conditions (Bagshaw & Trentham 1973; Bagshaw *et al.* 1975; Taylor 1977). The

Figure 1. Structure of the Dd myosin motor domain ADP·vanadate complex to show the location of mutations for introduction of fluorescent probes. Green, 25 kDa N terminal subdomain; red, upper 50 kDa subdomain; pink, lower 50 kDa subdomain; blue, 20 kDa C-terminal domain. The F129W mutation is at the entrance to the nucleotide-binding pocket, F239W is in switch 1 and W501 is a native tryptophan at the end of the relay loop. The cysteine mutations at S416 and N537 allow introduction of pyrene probes across the actin-binding cleft. Actin binds to loops on either side of the cleft region. The pathological E683K mutation is in the thiol helix. YFP and CFP are attached to the N and C termini. The diagram was prepared using PyMOL (http://www.pymol.org) and the 1VOM.pdb structure file (Smith & Rayment 1996).

ATP binding isomerization (step 2) was practically irreversible. Indeed, it was possible to synthesize small amounts of ATP bound to myosin by addition of high concentrations of P_i and ADP, showing all reactions after step 2 were at least moderately reversible (Goody *et al.* 1977; Mannherz *et al.* 1974; Sleep & Hutton 1980). The tight binding of ATP provides sufficient energy to dissociate actomyosin and the rapid kinetics shows that the route must pass through an A·M·ATP ternary complex because the spontaneous dissociation of the A·M complex is slow.

More recently these kinetic approaches have been applied to myosin II isolated from Dd (Ritchie *et al.* 1993; Kurzawa *et al.* 1997; Kuhlman & Bagshaw 1998). This system has the advantage of the preparation of mutant forms of myosin to probe its mechanism further (Ruppel & Spudich 1996). Furthermore several high-resolution structures of the Dd myosin motor domain have been determined by crystallography, so as to allow detailed correlation between structure and function of the various sub-domains within the myosin motor (Fisher *et al.* 1995; Smith & Rayment 1996; Gulick *et al.* 1997; Bauer *et al.* 2000; Reubold *et al.* 2003). In this overview we discuss our findings based on fluorescence signals obtained from tryptophan mutants, pyrene-labelled derivatives and GFP-labelled chimeras.

2. THE NUCLEOTIDE-BINDING POCKET

Wild-type Dd myosin shows little change in tryptophan fluorescence on nucleotide binding. However, the overall kinetic pathway can be represented by an equivalent scheme to equation (1.1), where the dagger represents an isomeric state that is practically optically silent in the high tryptophan fluorescence background of wild-type Dd

myosin (Kurzawa *et al.* 1997; Kuhlman & Bagshaw 1998):

$$M+ATP \underset{1}{\rightleftharpoons} M \cdot ATP \underset{2}{\overset{\rightharpoonup}{\leftharpoondown}} M^\dagger \cdot ATP \underset{3}{\rightleftharpoons} M^* \cdot ADP \cdot P_i$$
$$\text{\ding{7}}4 \qquad (2.1)$$
$$M+ADP \underset{7}{\rightleftharpoons} M \cdot ADP \underset{6}{\overset{\leftharpoonup}{\rightharpoondown}} M^\dagger \cdot ADP + P_i \underset{5}{\overset{\leftharpoonup}{\rightharpoondown}} M^\dagger \cdot ADP \cdot P_i$$

We retain the asterisk symbol to relate to the approximate fluorescence enhancement and, consequently, the major steady-state intermediate observed with skeletal myosin $M^{**} \cdot ADP \cdot P_i$ is equivalent to Dd $M^* \cdot ADP \cdot P_i$. The lack of signal on nucleotide binding can be accounted for by the lack of native tryptophan residues in the nucleotide-binding pocket, compared with skeletal myosin where residues equivalent to D113 and R131 are tryptophan. This proposal was tested by means of single-tryptophan-containing Dd constructs. The approach is viable because a mutant completely lacking tryptophan (so-called W−; Malnasi-Csizmadia *et al.* 2000) is active and therefore serves as a starting point for adding back tryptophan residues at any non-critical location (figure 1). Analysis of Dd mutants and single-tryptophan-containing mutants D113W and R131W, located near to the opening of the nucleotide-binding pocket, showed that they responded to nucleotide binding but not to hydrolysis (Kovacs *et al.* 2002). However, the amplitude (and direction in the case of R131W) could not account quantitatively for the signals observed in skeletal myosin, suggesting that other non-conserved residues contribute to the environment of these tryptophan residues and hence their response to nucleotide binding.

We also characterized a non-native mutant (W129+) where a conserved phenylalanine residue was substituted
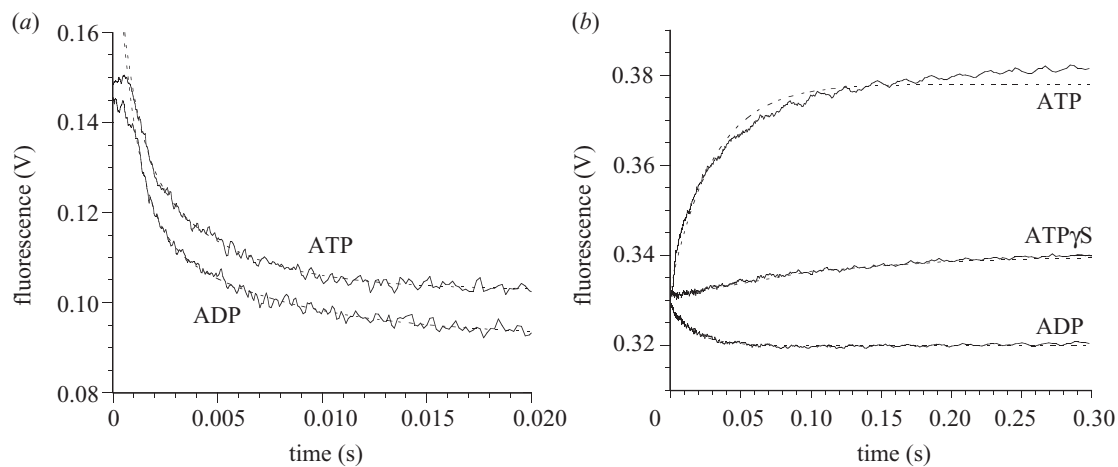
Figure 2. Stopped-flow records of nucleotide binding to W129+ and W501+ constructs. (*a*) Tryptophan fluorescence signal on mixing 250 μM ATP or 250 μM ADP with 2 μM W129+ construct. Fits to double exponential (dashed line) yield rate constants of 1200 s^{-1} and 240 s^{-1} for ATP and 1100 s^{-1} and 150 s^{-1} for ADP. These measurements were made with a 5 μl cell with 0.5 ms dead time (Kovacs *et al.* 2002). The curves are offset by 0.01 V for clarity. (*b*) Comparison of tryptophan fluorescence signal on mixing 1 mM ATP, 100 μM ATPγS or 100 μM ADP with 1 μM W501+ construct. Fits to a single exponential yielded rate constants of 33 s^{-1} for ATP, 66 s^{-1} for ADP and 9 s^{-1} for ATPγS. Conditions: 40 mM NaCl, 20 mM HEPES, 2 mM MgCl$_2$ at pH 7.5 and 20 °C.

with tryptophan and all native tryptophan residues were removed. This construct responded with a large fluorescence quench on binding ATP or ADP and proved useful in characterizing the initial isomerization events (Kovacs *et al.* 2002). As with skeletal myosin (Trybus & Taylor 1982), the isomerization was resolved into at least two steps (figure 2*a*,*b*), which appeared to be sequential and had rate constants that reached a maximum of *ca.* 1800 s^{-1} and 450 s^{-1} for ATP, and 1200 s^{-1} and 350 s^{-1} for ADP. Significantly, the amplitudes of the changes were the same for ATP and ADP, suggesting that W129 only responds to the initial binding events and not hydrolysis (figure 2*a*).

It is of interest to know if equivalent isomerizations occur when the myosin is bound to actin and whether they control the rate of dissociation of actomyosin by nucleotide. These experiments are not straightforward as the four tryptophan residues in actin dominate the net fluorescence signal and give a high background. Furthermore, experiments with tryptophanless myosin (W−) showed that there is a small (2–3%) apparent enhancement when actin and myosin associate which reverses on the dissociation step (Wakelin *et al.* 2002). This signal could arise from perturbation of actin tryptophan residues, although control experiments suggested that it is dominated by a light scatter artefact. Whatever the origin, the contribution must be considered when analysing signals for single tryptophan-containing myosin constructs.

ATP induces actomyosin dissociation with a rate constant of 70–100 s^{-1}, under our standard conditions (40 mM NaCl, 20 mM HEPES, 2 mM MgCl$_2$ at pH 7.5 and 20 °C), as determined by light scattering (Kuhlman & Bagshaw 1998; Conibear *et al.* 2003). In the case of ATP-induced dissociation of acto-W129+, the observed tryptophan fluorescence quench appeared coincident with the dissociation reaction. However, the signal had a large component from the expected dissociation reaction (based on the actoW− experiment) and therefore a small slightly faster phase from W129 itself would be difficult to resolve. The result with ADP was much less ambiguous. Here, a quench

in tryptophan fluorescence was observed with the same kinetics and absolute amplitude as observed with the W129+ construct in the absence of actin. In this case there was little dissociation of the actomyosin·ADP complex and that which occurred was on the seconds time-scale. A similar conclusion was reached when the slowly hydrolysable analogue ATPγS was used as a substrate. Here, the dissociation reaction was near complete, but the kinetics were much slower than those for ATP. These measurements showed that the changes in W129 fluorescence on ATPγS binding to acto-W129+ were slowed down by only twofold by actin and both phases (figure 2*a*) were complete before significant (less than 10%) dissociation occurred. These results imply W129 senses local events concerned with nucleotide binding and subsequent transitions are required to communicate with the actin-binding site to initiate the dissociation process (cf. switch 1 and cleft mutants discussed in § 3).

3. PROBES OF SWITCH 2 MOVEMENTS

Switch 2 is a region of myosin that interacts with the γ-phosphate of bound nucleotide, named originally for the corresponding region in G-proteins (Geeves & Holmes 1999). X-ray crystallography has revealed two positions of the switch 2 loop in myosin: open and closed. In the closed state the switch 2 loop moves 4 Å towards the γ-phosphate and makes direct contact with it via G457 (Fisher *et al.* 1995). In the case of Dd myosin II, switch 2 comprises residues 454–459. Alanine scanning shows that residues D454, G457, F458 and E459 are essential for actin-activated ATPase and *in vitro* motility (Sasaki *et al.* 1998). Our attempts to replace F458 with W also led to inactive protein (Wakelin *et al.* 2002). Preliminary studies with an F461W mutant showed that this protein was active and the fluorescence responded to ADP and ATP binding, but further analysis is required to establish the kinetics of the signal at high nucleotide concentrations (Wakelin *et al.* 2002).

Probing events at the nucleotide-binding site by mutagenesis of switch 2 is likely to cause some perturbation to

the mechanism. Fortunately a naturally occurring trypto-phan, located at the end of the relay helix attached to switch 2, provides large signals that are sensitive to the nucleotide state. Early studies of vertebrate myosin showed that part of the protein fluorescence enhancement was coincident with the hydrolysis step (Bagshaw *et al.* 1974; Johnson & Taylor 1978). There is now abundant evidence that this signal arises from a conserved tryptophan residue (Dd W501 (Batra & Manstein 1999; Malnasi-Csizmadia *et al.* 2000), skeletal W510 (Park & Burghardt 2000) and smooth myosin W512 (Onishi *et al.* 2000; Yengo *et al.* 2000)). By using a single tryptophan construct (i.e. a sub-stitution of the other native tryptophans with phenylala-nine) the signal to background is increased and the origin of the signal is defined unambiguously. In addition, we found that, in the case of Dd W501+ construct, nucleotide bind-ing caused a quench in fluorescence while the subsequent steps, associated with hydrolysis, caused a large enhance-ment (Malnasi-Csizmadia *et al.* 2000).

The fluorescence change on mixing ATP with the W501+ construct at 20 °C appears deceptively simple (figure 2b). The enhancement is fitted reasonably well by a single exponential whose rate constant increases with [ATP] up to a limiting value of *ca.* 30 s^{-1}. This was assumed to be a measure of the sum of the forward and reverse rate constants for hydrolysis (step 3, equation (2.1)). In contrast to the 80% enhancement in W501 fluorescence induced by ATP, ADP binding induced a 15% quench and the kinetics increased with [ADP] to at least 400 s^{-1}. However, AMP·PNP and ATPγS binding induced neither a quench nor a substantial enhancement in W501 fluorescence at 20 °C (Malnasi-Csizmadia *et al.* 2000). These results could be rationalized after consider-ation of nucleotide-binding data obtained at low tempera-tures (2–10 °C). Here, all nucleotides showed an initial quench in W501 fluorescence, followed by a variable enhancement dependent on the degree of hydrolysis. It was proposed that the enhancement of W501 fluorescence, and hence switch 2 movement, was not directly coupled to hydrolysis (Malnasi-Csizmadia *et al.* 2000). Rather nucleotides with a γ-phosphate group allowed rapid but reversible closure of switch 2 but hydrolysis was required to pull the equilibrium over to give a predominant closed state. The nucleotide binding and hydrolysis mechanism of equation (2.1) was therefore extended:

$$M+ATP \underset{}{\overset{1}{\rightleftharpoons}} M \cdot ATP \underset{}{\overset{2}{\rightleftharpoons}} M^{\dagger} \cdot ATP \underset{}{\overset{3a}{\rightleftharpoons}} M^{*} \cdot ATP \underset{}{\overset{3b}{\rightleftharpoons}} M^{*} \cdot ADP \cdot P_i$$

$$\left\Vert 4 \right. \qquad (3.1)$$

$$M+ADP \underset{}{\overset{7}{\rightleftharpoons}} M \cdot ADP \underset{}{\overset{6}{\rightleftharpoons}} M^{\dagger} \cdot ADP + P_i \underset{}{\overset{5}{\rightleftharpoons}} M^{\dagger} \cdot ADP \cdot P_i$$
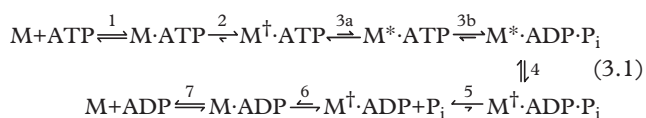
where the dagger represents a 15% quench (and barely detectable in the native Dd motor domain where the relative signal is reduced fourfold by the non-responsive tryptophans) and the asterisk represents an 80% enhance-ment in W501 fluorescence (note the precise amplitudes dependent on the bandpass width of the emission channel of the fluorimeter). In structural terms, the dagger represents the open state defined by the crystal structure with ADP (1MMA.pdb (Gulick *et al.* 1997)) and the asterisk represents the closed state defined by analogues of the myosin-products complex (e.g. M*·ADP·Vi, 1VOM.pdb (Smith & Rayment 1996) and 1MND.pdb

M*·ADP·AlF$_4$ (Fisher *et al.* 1995)), which give a large fluorescence enhancement (Malnasi-Csizmadia *et al.* 2000). Step 2 has been resolved into at least two phases (2a and 2b; but the overall flux is limited by 2b (Kovacs *et al.* 2002)). Step 3a is rapid compared with steps 2b and 3b and remains almost in equilibrium (Malnasi-Csizmadia *et al.* 2001). Note the unfavourable equilibrium of step 3a. At 20 °C the value of K_{3a} for nucleoside triphosphates is *ca.* 0.2, thus the weighted fluorescence yield from the com-bined M†·ATP and M*·ATP states is +80*0.2/1.2 − 15*1/1.2 ≈ 0%. This cancellation of signal accounts for the fact that there is neither a significant initial burst associated with M*·ATP nor a quench associated with M†·ATP for-mation when ATP binds to the W501+ construct at 20 °C. Only a single phase is observed as hydrolysis (step 3b) pro-ceeds and pulls the net equilibrium towards the closed state, with an apparent rate constant of 30 s^{-1}. The actual hydrolysis rate constant, k_{3b}, is about five times faster than that observed because it is preceded by an unfavourable equilibrium constant K_{3a}. The sensitivity of the fluores-cence profile to the values of K_{3a} and k_{3b} is illustrated by the simulations shown in figure 3.

At low temperatures, K_{3a} is smaller and also the hydroly-sis reaction is less favourable so that quench arising from M†·ATP becomes visible as a brief transient (Malnasi-Csizmadia *et al.* 2000, 2001). AMP·PNP also allows lim-ited formation of the closed state, but the lack of hydrolysis ($K_{3b} = 0$) results in either a small net fluorescence quench or enhancement depending on the precise value of K_{3a}. Increasing temperature increases K_{3a}, as observed with other nucleotides. ATPγS, however, does show a slow and limited hydrolysis reaction that increases the net equilib-rium of step 3, but the open state is dominant throughout and the net fluorescence signal remains close to that of the initial apo state (figure 2b). Direct evidence for the exist-ence of an M*ATP state in equilibrium with the M†·ATP state came from relaxation techniques where temperature- and pressure-jump methods revealed that $k_{3a} + k_{-3a}$ was *ca.* 1000 s^{-1} at 20 °C for ATP and AMP·PNP (Malnasi-Csizmadia *et al.* 2001; Urbanke & Wray 2001). Equation (3.1) is in accord with structural studies, which suggest that switch 2 must close before hydrolysis can proceed (Geeves & Holmes 1999). It is clear from our studies that the pres-ence of nucleoside triphosphate at the active site does not allow a stable complex formation between the switch 2 resi-dues and γ-phosphate, but one in which the switch 2 region fluctuates between the open and closed states on a milli-second time-scale until hydrolysis occurs. Once hydrolysis occurs the closed switch 2 state is favoured but this reaction is also reversible on the hundreds of milliseconds time-scale and so the open state can be re-established by reversal from the M*·ADP·P$_i$ state to the M†·ATP state many times before the products are eventually released. This accounts for the incorporation of nearly four oxygen atoms from water into the product phosphate (i.e. intermediate ^{18}O exchange). The dynamic nature of the switch 2 region is also suggested by the fact that crystals of the Dd M·ADP·BeFx complex can be trapped in both the open and closed states (Geeves & Holmes 1999).

The W501 signal has proved a useful probe for the open–closed transition in the context of P$_i$ binding (Wake-lin *et al.* 2002). Previous studies provided evidence of reversibility of the combined steps 3, 4 and 5 (equation
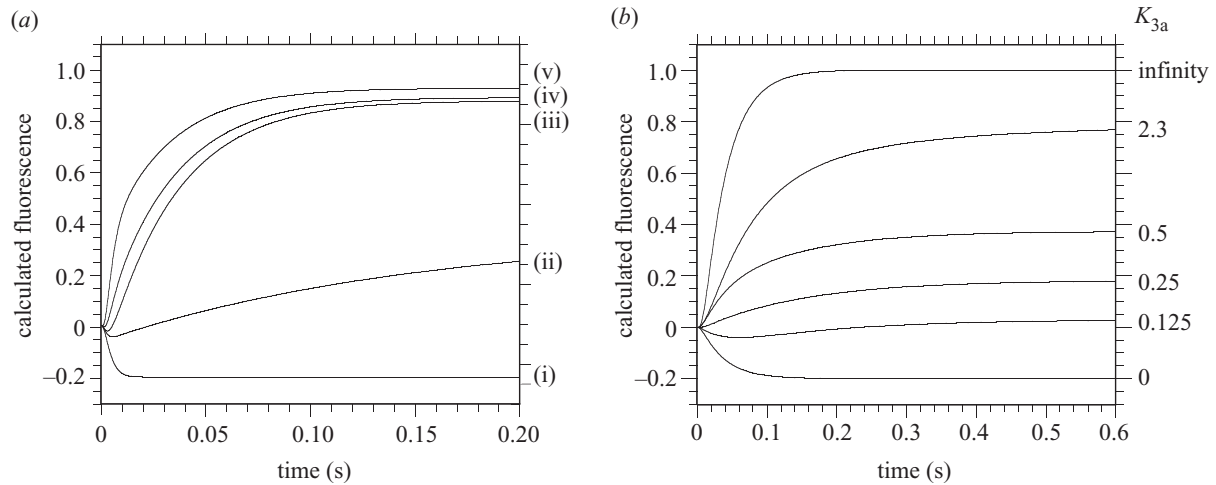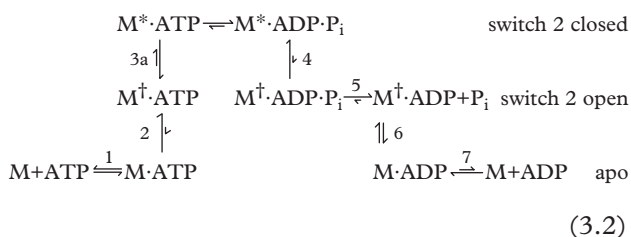
(a)

(b)

Figure 3. Simulations to show the effect of K_{3a} (open-closed equilibrium) on W501 fluorescence induced by different nucleotides. Simulations were performed using Berkeley Madonna (www.berkeleymadonna.com) for the scheme shown in equation (3.1) with varying values for K_{3a} and k_{3b}. $M^{\dagger}$ states were weighted with a 20% quench and M^* states 100% enhancement, relative to apo M. (a) Simulations to represent the profiles on mixing ADP or ATP with the W501+ construct at high and low temperatures (Malnasi-Csizmadia *et al.* 2000, 2001). The following rate constants were fixed at $k_{2a} = 1500\ s^{-1}$, $k_{2b} = 450\ s^{-1}$, $k_{-3b} = 4\ s^{-1}$, $k_4 = 0.05\ s^{-1}$. (i) $K_{3a} = 0$ represents the case with ADP at all temperatures. (ii) $K_{3a} = 0.15$, $k_{3b} = 20\ s^{-1}$ represents ATP at 5 °C where a small transient quench is observed. (iii) $K_{3a} = 0.2$, $k_{3b} = 180\ s^{-1}$, (iv) $K_{3a} = 0.4$, $k_{3b} = 100\ s^{-1}$, and (v) $K_{3a} = 1$ and $k_{3b} = 60\ s^{-1}$ all represent ATP at near 20 °C to give an effective hydrolysis rate of 30 s^{-1}. Note in (iii) there is a small lag and in (v) there is a clear biphasic enhancement, while in (iv) the profile is close to a single exponential as is observed at 20 °C. (b) Simulations to show the effect of K_{3a} equilibrium constant with fixed hydrolysis rate constants, $k_{3b} = k_{-3b} = 4\ s^{-1}$, appropriate to ATPγS. The following rate constants were fixed at $k_{2a} = 450\ s^{-1}$, $k_{2b} = 30\ s^{-1}$, $k_4 = 0.5\ s^{-1}$. The observed transient (figure 2b) indicates a K_{3a} value of *ca.* 0.25 for ATPγS in the absence of actin.

(1.1)), with skeletal myosin from the level of incorporation of $^{32}P_i$ into the M^*·ATP state (Goody *et al.* 1977). P_i binding to the apo W501+ construct gave a 10% fluorescence quench, similar to ADP. However, when P_i was added to W501+ in the presence of ADP, an enhancement was observed, indicative of formation of the M^*·ADP·P_i state. At 30 mM P_i, the enhancement was *ca.* 25% that of the signal for M^*·ADP·P_i during the steady-state, but this concentration was well below saturation (Wakelin *et al.* 2002). Unfortunately, non-specific ionic strength effects preclude accurate determination of the K_d from the amplitude of enhancement as a function of $[P_i]$. However, the data suggest that the equilibrium of step 4 (equation (3.1)) lies towards the M^*·ADP·P_i state, with an overall equilibrium constant $K_4 K_5$ for P_i binding of *ca.* 90 mM. Rearranging equation (3.1) emphasizes the relationship of conformation to kinetic states (i.e. the † to * fluorescence states are assumed to equate to the open and closed-states of switch 2, respectively).

$$M^*\text{·}ATP \rightleftharpoons M^*\text{·}ADP\text{·}P_i \qquad \text{switch 2 closed}$$

scheme with 3a, 4, 2, 5, 6, 7, 1 labels:

$M^{\dagger}$·ATP $M^{\dagger}$·ADP·P_i $\overset{5}{\rightleftharpoons}$ $M^{\dagger}$·ADP+P_i switch 2 open

$M+ATP \overset{1}{\rightleftharpoons} M\text{·}ATP$ $\qquad$ $M\text{·}ADP \overset{7}{\rightleftharpoons} M+ADP$ apo

(3.2)

This scheme indicates the need for switch 2 to open before P_i release, i.e. the $M^{\dagger}$·ADP·P_i state exists on the pathway. The evidence for this state was initially proposed

on the basis of the weak binding but rapid kinetics of P_i binding to M in the presence of ADP (Bagshaw & Trentham 1974). However, it is also possible that the $M^{\dagger}$·ADP state is in equilibrium with a very low concentration of M^*·ADP and the route is M^*·ADP·P_i $\leftrightarrow$ M^*·ADP $\leftrightarrow$ $M^{\dagger}$·ADP. The role of switch 1 movement in P_i release is discussed below.

It is of interest to determine the influence of actin on the switch 2 open–closed transitions. This is not straightforward because ATP induces rapid dissociation of the acto-myosin complex. When acto-W501+ construct is mixed with ATP, the predominant phase in tryptophan fluorescence is an enhancement at *ca.* 20 s^{-1} that occurs after dissociation is near complete. This observation simply confirms the Lymn & Taylor (1971) postulate that hydrolysis occurs subsequent to the dissociation step and has practically the same kinetics as for myosin alone. However, the nucleotide-binding isomerizations cannot be resolved from the dissociation phase, and so the influence of actin on the open–closed transition (step 3a) cannot be determined unambiguously (i.e. the ternary A·$M^{\dagger}$·ATP and A·M^*·ATP complexes do not exist in sufficient concentration during their transient formation to determine their ratio).

This problem was overcome using ATPγS as the dissociating nucleotide, where studies with the W129+ construct showed that the nucleotide binding events were complete before significant dissociation occurred. At 20 °C, ATPγS binding to the W501+ construct gives a small net enhancement over the first 30 ms indicative of a K_{3a} value of 0.25 (figure 2b cf. figure 3b) and a slow reversible hydrolysis reaction ($k_{3b} \approx k_{-3b} \approx 4\ s^{-1}$). In the presence of actin the net enhancement was less and
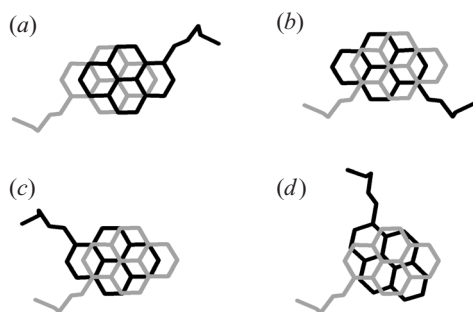
Figure 4. Pyrene ring overlap to form excimers or a quenched dimer. Pyrene excimers require the pyrene rings to associate with a precise stagger of 1.3 Å as in (*a–c*). Nevertheless there are six combinations of cysteine derivatives that allow excimer formation and result in separation of the α carbon of the cysteine residues from 0 to 23 Å. Shown here are (*a*) anti-parallel *trans* with maximum stagger; (*b*) anti-parallel *cis* with minimum stagger; and (*c*) parallel *trans* configurations. Pyrene rings that associated at other angles or stagger, as in (*d*), result in quenching of fluorescence emission. Modelling indicates that the 50 kDa cleft in a open state could only accommodate the two pyrene rings in an anti-parallel configuration, whereas a closed cleft could only accommodate a parallel configuration.

comparison with figure 3*b* indicated that K_{3a} was reduced by about twofold. Thus actin has a minor effect on the open-to-closed transition, at least in the case of the myosin.nucleoside triphosphate complex. From thermo-dynamic balance, actin must bind up to twofold more tightly to the open state relative to the closed state.

In the case of ADP, the open state predominates such that equivalent K_{3a} open-to-closed transition, if it occurs, has an equilibrium constant of less than 0.05 because the M^*·ADP state is undetectable. Actin had no effect on the observed ADP-induced quench of W501 fluorescence such that this limit of K_{3a} remained in the presence of actin. The lack of any marked effect of actin on the equilibrium of the open-to-closed transition has important implications for the product release mechanism and its coupling to the putative lever arm swing (see below). These measurements reflect the unloaded condition. Clearly for values of K_{3a} *ca.* 1 (i.e. 0.1 to 10) then load on the lever arm would greatly perturb the equilibrium distribution of states.

4. PROBES OF SWITCH 1 MOVEMENTS

Switch 1 is another conserved region of myosin that inter-acts with the nucleotide and again named by homology with the corresponding region in G-proteins. In Dd myosin it comprises residues 233–240 and alanine scanning showed that residues N233, S237 and R238 were essential for *in vitro* motility (Shimada *et al.* 1997). Until 2003, all high-resolution crystal structures of myosin where switch 1 was resolved showed that it was in the so-called closed state where interactions occurred with the γ-phosphate and Mg^{2+} ion when present. However in 2003, two apo myosin structures were solved where it was reported that switch 1 had moved towards the open position (Coureux *et al.* 2003; Reubold *et al.* 2003). In the myosin V structure (Coureux *et al.* 2003) it appeared that switch 1 movement was coupled to closure of the cleft between the upper and lower 50 kDa subdomains, and thus provided a potential

mechanism whereby actin binding controls events at the nucleotide-binding site and *vice versa*. To probe the switch 1 region we recently constructed two single tryptophan mutants, W239+ and W242+ in which phenylalanine resi-dues were replaced.

Preliminary studies show that both mutants appear to retain the basic ATPase pathway, although the nucleotide dissociation from actin is slowed down by an order of mag-nitude compared with the wild-type motor domain. This property is actually advantageous in that it allows better resolution of the kinetics without having to resort to ATPγS, as described above for the W129+ and W501+ constructs. In the case of W239+, ATP interaction causes a marked blue shift and quench in fluorescence, while ADP binding causes a similar shift but with a smaller quench. The kinetics of ATP interaction followed a single exponen-tial whose rate constant increased linearly with [ATP]. However, in the presence of actin the profile was markedly biphasic, with the slow second phase closely matching the dissociation reaction. Thus, unlike the profiles from W501+ and W129+, which are changed by less than three-fold, the kinetics of the nucleotide-induced response of W239+ are markedly altered by actin.

Actin binding to the W239+ construct in the absence of nucleotide caused little change in fluorescence. Although further measurements are required, the data obtained to date suggest that the apo myosin has switch 1 in an open state or in a dynamic equilibrium with a significant popu-lation in the open state. ATP binding in the absence of actin causes rapid closure of switch 1 with a concomitant quench in fluorescence. The transients from W242+ that we have measured are comparable to those of W239+, sug-gesting that the tryptophan signals are reporting on the switch 1 loop as a whole rather than the local motion of the side chains.

Some of the structures for apo states of myosin have been solved by crystallization from solvents containing high sul-phate concentrations (Rayment *et al.* 1993*b*; Houdusse *et al.* 2000). The presence of sulphate may stabilize the switch 1 closed state. It is of interest to note that ammonium sul-phate caused a quench in W239 fluorescence, almost as large as with ATP. Sulphate occupancy at the β- or γ-P_i position may result in switch 1 closure.

5. PROBES OF THE ACTIN-BINDING CLEFT

The crystal structures of myosin reveal a large cleft between the upper and lower 50 kDa subdomains. Early on it was suggested that this cleft might close on binding to actin and this process could constitute the final step in a multistep docking of myosin from an initial weak binding state to a strong binding state (Rayment *et al.* 1993*a*). This concept has been developed further in the light of recent crystal structures in which switch 1 was in the open state and the upper 50 kDa domain had undergone a rotation and par-tial closure relative to previous structures (Holmes *et al.* 2003). The coupling between switch 1 and the actin-binding site via cleft movements provides a means of communi-cation between the nucleotide site and actin site.

To test these concepts in solution we engineered pairs of cysteine residues across the cleft in a construct that was deficient in native cysteine residues (the buried C655 was retained; Shih *et al.* 2000). Fluorescent and spin-
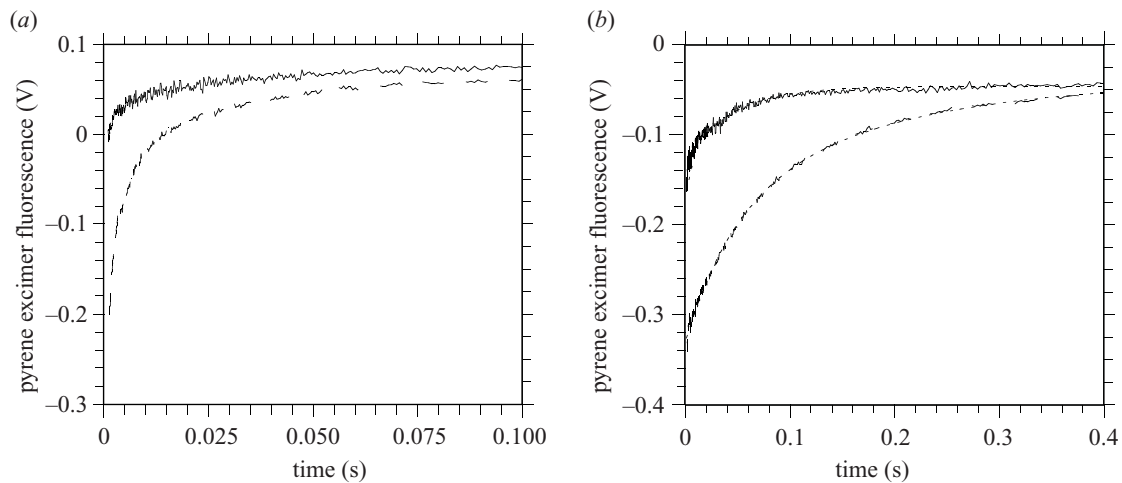
Figure 5. ATP and ATPγS binding to pyrene-labelled S416C/N537C construct. (*a*) 500 μM ATP was mixed with 1 μM pyrene-labelled construct in the absence (top curve) and presence (bottom curve) of 2 μM actin. Excimer fluorescence was monitored with 365 nm excitation and an GG455 nm cut-off emission filter. Biexponential fits gave 440 s^{-1} (0.058 V) and 25 s^{-1} (0.045 V) in the absence of actin and 505 s^{-1} (0.27 V) and 25 s^{-1} (0.13 V) in its presence. (*b*) Similar experiment but with ATPγS to yield 950 s^{-1} (0.088 V) and 23 s^{-1} (0.083 V) in the absence of actin and 22 s^{-1} (0.13 V) and 6 s^{-1} (0.15 V) in its presence. The amplitudes were corrected for a dead time of 1.5 ms for the 20 μl cell. Conditions: 40 mM NaCl, 20 mM HEPES, 2 mM MgCl$_2$ at pH 7.5 and 20 °C.

label probes have been attached to the cleft cysteines to enable cleft movements to be monitored. When pyrene was attached to the S416/N537C construct, using the N-1-iodoacetamide derivative, the emission spectrum showed a dominating contribution from the pyrene excimer state (Conibear *et al.* 2003). This feature shows that the pyrene rings attached to the two cysteine residues pair up with a 3.5 Å separation and 1.3 Å stagger, as required for excimer emission (figure 4). Fluorescence lifetime measurements and the excitation wavelength-dependent emission spectra both indicated that the pyrene rings formed ground-state dimers. Addition of actin to this labelled preparation caused a 60% reduction in excimer emission intensity with only a small increase in monomer emission. These data suggest that the cleft moves and that the pyrene rings reorient to favour the formation of the quenched dimer state (Lehrer 1997). Although such measurements do not provide a quantitative measure of the extent or direction of movement, they did allow the kinetics of the movement to be followed with millisecond time resolution (Conibear *et al.* 2003).

ATP addition to the acto-pyrene-S416/N537C construct caused a reversal of the fluorescence quench with biphasic kinetics (figure 5*a*). The fast phase in pyrene excimer fluorescence was at least as fast as the rate of dissociation, as measured by light scattering, suggesting that the movement that was monitored was on the pathway to dissociation. ATP addition to the pyrene-labelled motor domain in the absence of actin gave a small increase in pyrene excimer fluorescence but with similar kinetics. If the fluorescence change was linearly related to cleft opening, then these data suggest that in the apo form the cleft is largely open or is in dynamic equilibrium with a cleft open form predominating. Together with the results from switch 1 probes above, this suggests that the switch 1 and cleft might be uncoupled in the apo myosin state (i.e. both switch 1 and the cleft are open). Alternatively, because the

fluorescence signals are likely to be highly nonlinear, it is possible that W239 only senses the initial opening of switch 1 and/or pyrene excimer preferentially senses the initial opening of the cleft.

ATPγS binding to the pyrene-labelled motor domain in the absence of actin also gave a small increase in pyrene excimer fluorescence with kinetics and amplitudes within a factor of 2 that obtained with ATP. However, in the presence of actin, both the pyrene excimer signal (figure 5*b*) and the light scatter signal were an order of magnitude slower (Conibear *et al.* 2003). This result contrasts with the signals from W129 and W501, where tryptophan fluorescence response was slowed less than threefold by actin, while the dissociation reaction was two orders of magnitude slower. ADP binding caused a more limited and much slower reversal of the quench of acto-pyrene-labelled motor domain fluorescence, in line with only partial and slow dissociation. These data added weight to the argument that pyrene excimer fluorescence is monitoring a cleft movement that is a requirement for actin dissociation.

6. PROBES OF THE LEVER ARM

Lever arm movement has been assessed for proteins in solution by the use of FRET and luminescence resonance energy transfer probes attached to the N and C termini of the motor domain (Suzuki *et al.* 1998; Shih *et al.* 2000; Xiao *et al.* 2003). Sutoh and colleagues (Suzuki *et al.* 1998) constructed a GFP-Dd myosin motor-BFP chimera and showed that FRET between the BFP and GFP probes depended on the state of the nucleotide bound to the ATPase site. We repeated this kind of experiment but with CFP and YFP as the donor and acceptor, respectively. In the apo state this construct showed extensive FRET, but on ATP addition the change in FRET was small and could not be accurately determined. A difficulty in detecting small changes in FRET during steady-state spectral scans could result from CFP bleaching during the scan. The analogous
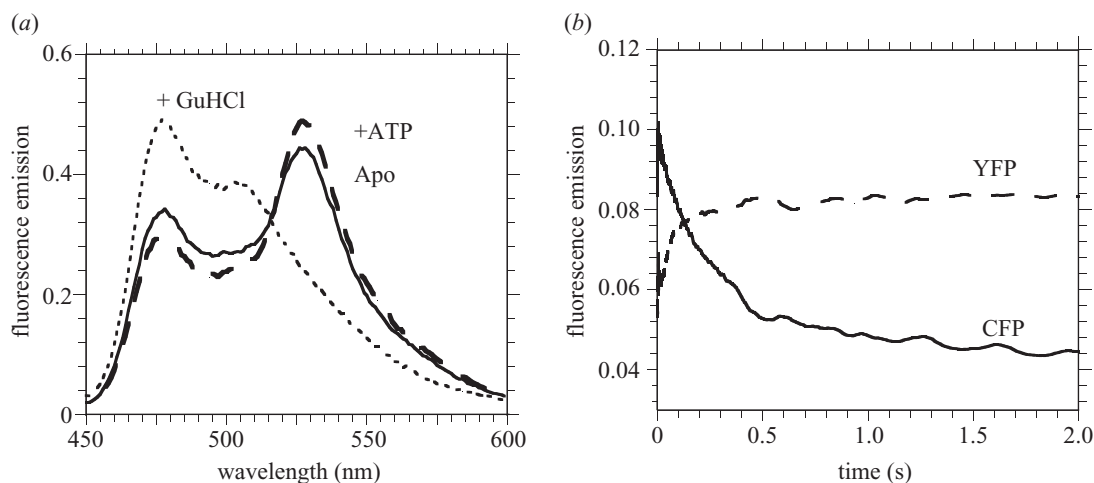
Figure 6. ATP-induced changes of FRET in YFP-Dd W501+ -CFP constructs. (*a*) Emission spectra on excitation of CFP (436 nm) showing FRET to YFP (527 nm peak). Solid line is YFP-Dd 501+ -CFP construct with two GGG linkers (see text) in 1 M KCl, 40 mM NaCl, 20 mM HEPES, 2 mM MgCl$_2$ at pH 7.5 and 20 °C. Addition of 0.7 mM ATP caused a 10% enhancement in the YFP emission and a 15% quench in CFP emission. In the absence of the high KCl concentration the FRET changes on ATP addition were less than 5%. On addition of 1 M guanidine hydrochloride (GuHCl), the YFP emission peak was absent, leaving the double peaked emission of CFP (480 and 506 nm). This indicated that the Dd W501+ moiety had denatured but the CFP (and presumably YFP) remained folded but the fluorophores were now separated by more than 10 nm. (*b*) Dual wavelength stopped-flow record on mixing 5 μM ATP with 1 μM YFP-Dd 501+ -CFP construct, containing a single GGG linker to CFP, in 40 mM NaCl, 20 mM HEPES, 2 mM MgCl$_2$ at pH 7.5 and 20 °C. Excitation was at 438 nm, while CFP emission was recorded through a combined filter set (GG450+ IK505, Comar Instruments, Cambridge), giving 485±25 nm bandpass and YFP was selected with an OG530 nm cut-off filter.

bleaching of BFP would also account for an absence of the significant BFP de-quenching in the FRET experiments of Suzuki *et al.* (1998). Increasing the ionic strength with KCl reduced the overall extent of the FRET in the apo state but rendered the FRET signal sensitive to nucleotide. The decrease in FRET could arise from: (i) disruption of non-specific electrostatic interactions between the fluorescent proteins which might cause dimerization of CFP and YFP when brought into close contact, or (ii) a reduction in absorbance of YFP on binding chloride ions that make it a weaker acceptor (Wachter & Remington 1999). Interestingly, at high ionic strength, ATP addition caused a 10% increase in YFP fluorescence emission when excited via the CFP donor (figure 6*a*), which is in the *opposite* direction to that reported by Suzuki *et al.* (1998) for the equivalent measurement with the BFP-myosin-GFP chimera.

Distance determination from FRET data between fluorophores based on the GFP is complicated by the slow rotation of these probes such that orientation effects are likely to contribute, if not dominate, the extent of FRET. Steady-state experiments for CFP and YFP yield values for anisotropy of *ca.* 0.3 (Wakelin *et al.* 2002; Wakelin & Bagshaw 2003) and argue that the proteins are relatively static on the time-scale of their fluorescent lifetime (*ca.* 3 ns), as expected from their molecular volume. It is likely that the difference in the direction of the FRET signals on ATP addition for the GFP-myosin-BFP construct (Suzuki *et al.* 1998) compared with the YFP-myosin-CFP construct arises from the different orientations that the probes take on relative to the myosin. This, in turn, depends on the nature of the linking amino acids. In the original publication, Suzuki *et al.* (1998) stated that a triple glycine (GGG) linker was inserted between the probes and the myosin, but

subsequently (Sasaki *et al.* 2003) it was reported that the GFP was attached via a GPG linker. In our initial construct we used two GGG linkers, but the sequence still differs from that of Suzuki *et al.* (1998) because of a slightly different cloning strategy. We also used the W501+ construct as the motor domain. Our construct, with a C-terminal His-tag, is:

(YFP)-*GGGMD*-**PIHDR**...(*Dd* motor domain)...

EAREQR-*LGSGGG*-(CFP)-*RDAL*H$_8$,

where residues in italics correspond to the linker regions and those in bold to the myosin W501+ sequence. We also prepared a construct in which the glycine residues were removed from the YFP linker to give a potentially more rigid N-terminal probe

(YFP) · DELYK*D***PIHDR**...(*Dd* motor domain)...

EAREQR-*LGSGGG*-(CFP)-*RDAL*H$_8$,

where DELYK is the C terminus of the native YFP sequence. At physiological ionic strength, this construct showed small (5% or smaller) changes in FRET that were difficult to define accurately in steady-state spectral measurements but were readily be determined in stopped-flow measurements with dual wavelength emission detection (figure 6*b*). Again addition of ATP caused an increase in the FRET efficiency, which recovered after hydrolysis to ADP.

From these results we conclude that FRET between fluorescent probes attached to the N and C termini of the myosin motor domain does provide evidence of lever arm movement in response to nucleotide occupancy at the active site. It is difficult, however, to convert the observed changes in FRET efficiency to absolute distances, owing to

working stroke

A·Moc·D ⇌ A·Moo·D → A·Moo

A·Moo ⇌(1) A·Moo·T → A·Moc·T   A·Moc·D·P ⇌ A·Moo·D·P   strong binding states

(2)

A·Mco·T ⇌(3a) A·Mcc·T ⇌(3b) A·Mcc·D·P ⇌ A·Mco·D·P   weak binding states

return stroke   hydrolysis   futile cycle
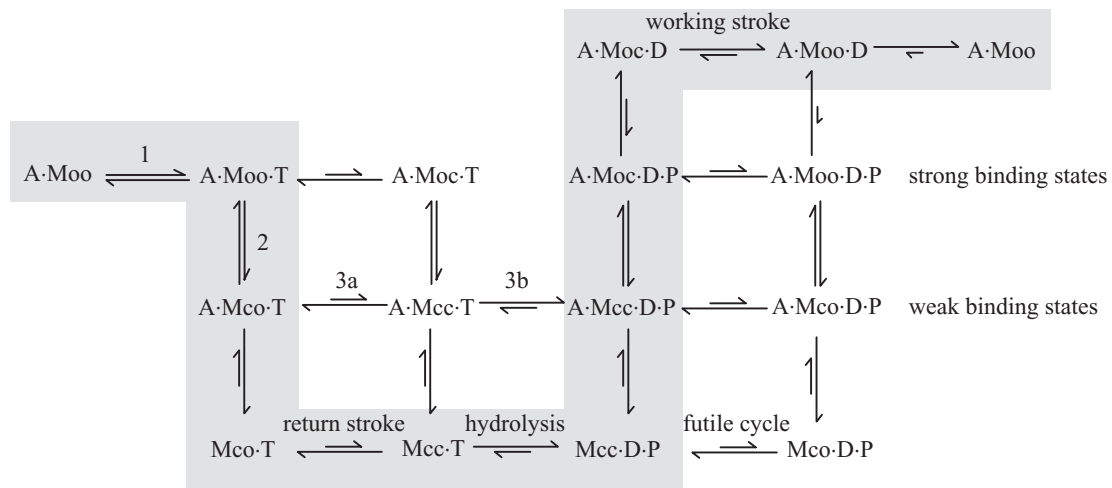
Mco·T ⇌ Mcc·T ⇌ Mcc·D·P ⇌ Mco·D·P

Figure 7. The actin-activated ATPase pathway and its possible coupling to the opening and closing of switch 1 and 2. The letters o and c refer to an open- or closed-switch state, respectively, with switch 1 preceding switch 2; T, ATP; D, ADP; P, P_i. This model assumes that the primary effect of actin is on the rate and position of the switch 1 closed–open transition (i.e. the Moc·D·P state is insignificant and omitted from the pathway). However, actin is assumed to have no significant effect on equilibrium of the switch 2 open-to-closed transition compared with the equivalent reaction in the absence of actin. The enhanced fluorescence state (denoted by an asterisk in the text) is assumed to be related to switch 2 closing and the lever arm in the pre-power stroke position. Switch 2 opening is coupled to the lever arm swing and the working stroke. Switch 1 closing results in a weak actin binding state. The dominant route that minimizes futile cycling is highlighted in grey.

uncertainties in the relative orientations of the probes. Nevertheless, the approach provides a useful empirical signal. Suzuki *et al.* (1998) showed that the maximum observed rate constant for the FRET change, on mixing with ATP, correlated with the maximum rate constant recorded for tryptophan fluorescence, i.e. the apparent hydrolysis step. Further studies are required to demonstrate whether the FRET probes monitor the rapid open-to-closed transition directly.

Actin addition to the YFP–myosin–CFP construct gave a small apparent quench in both fluorophores but no significant change in FRET. This result argues that there is no change in lever arm conformation when the apo myosin state binds to actin in the rigor state. The finding agrees with crystallographic and electron microscopy data that required no change to the light-chain binding domain angle relative to the head when the molecular structures were docked into the electron density of decorated filaments.

7. CORRELATION OF MYOSIN MOVEMENTS TO THE CROSS-BRIDGE STROKE

Site-directed mutagenesis is a powerful tool for testing the roles of individual amino acids or segments of sequence so as to define structure–function relationships in myosin (Ruppel & Spudich 1996). Here, we have taken a different tack of using this tool to introduce fluorescence probes into the myosin molecule with minimal perturbation of function. Mutagenesis is invariably accompanied by a change in the rate constants of some steps. However, provided the overall features of the Lymn–Taylor mechanism are preserved (i.e. actomyosin dissociation by ATP and actin activation of the basal myosin ATPase rate) then useful information is to be gleaned.

Structural and kinetic events associated with ATP binding to myosin II and the mechanism of actomyosin dissociation can now be correlated in a reasonably satisfying way (equation (3.2); figure 7). The apo myosin state has at least a partly open switch 1 and fully open switch 2 state. ATP binding occurs rapidly and local rearrangements at the nucleotide site, as sensed by W129, occur at 1000 s^{-1} (step 2a) and 500 s^{-1} (step 2b). In the absence of actin, switch 1 also closes on this time-scale (more than 800 s^{-1}), as shown by W239 and W242 fluorescence. The slower transition (step 2b) sensed by W129 appears to be detected by W501 fluorescence to give a small quench in the latter, but the structural significance of this is not clear. Immediately after this isomerization, and in near equilibrium with it, is the switch 2 open-to-closed transition. This transition appears to be a major conformational rearrangement that is transmitted from switch 2 to the lever arm via the relay helix. However, with nucleoside triphosphates at the active site, switch 2 closure is not favoured ($K_{3a} < 1$) and the predominant state is M†·ATP until the hydrolysis reaction (step 3b) ensues and pulls the net equilibrium of step 3 over to the closed state, M*·ADP·P$_i$. Conversely, hydrolysis is not possible except when the switch 2 temporarily closes to give the M*·ATP state. Switch 2 movement appears necessary to stabilize a water molecule in line with the γ-P$_i$ group which will allow hydrolysis (Fisher *et al.* 1995).

Addition of actin to the apo myosin state induces closure of the myosin 50 kDa cleft to form the tightly bound rigor state (figure 7; A.Moo, where the first and second 'o' refer to the status of switch 1 and switch 2, respectively). This process is accompanied by the full opening of switch 1. ATP binding to actomyosin follows a similar path to that of myosin alone, except that closure of switch 1 is slowed down, presumably because it has to work against the antagonistic effect of bound actin. Thus the local changes sensed by W129 are relatively unaffected by actin, whereas the switch 1 probes, W239 and W242, respond with a slow second phase in the presence of actin. Closing of switch 1, drives the opening of the 50 kDa cleft and disrupts the tight binding of actin. Actin dissociation now ensues to yield a

near equilibrium mixture of $M^\dagger \cdot ATP$ and $M^* ATP$ (i.e. Mco·T and Mcc·T in the nomenclature of figure 7). The switch 2 open-to-closed transition is only marginally affected by actin, but undergoes a major shift during the hydrolysis reaction that occurs subsequent to dissociation. Nevertheless, the formation of a limited fraction of $A \cdot M^* \cdot ATP$ (i.e. A·Moc·T and A·Mcc·T) gives rise to the possibility of a reverse working stroke before dissociation. This is not likely to be the major pathway, given the value of K_{3a} and the slightly more favourable binding of actin to the switch 2 open state. If 10% of the cross-bridges took that route, it would be just below the limits of detection of a reverse working stroke in optical trap experiments (Steffen *et al.* 2003; Steffen & Sleep 2004).

The events subsequent to hydrolysis are more difficult to study, because the key intermediates correspond to relatively low occupancy states. There is strong evidence that P_i leaves before ADP and the crystal structures indicate that P_i exits via a different route from that of the nucleotide for steric reasons (Yount *et al.* 1995). Previously it was suggested that actin might favour switch 2 opening (and hence lever arm movement) to activate the release P_i (Geeves & Holmes 1999). However, our data indicate that actin has only a minor effect on the equilibrium of the switch 2 open–closed transition, at least in the case of the nucleoside triphosphate state. What alternative mechanisms for actin activation can be offered?

The sequence of events in product release is initiated by the weak binding of the $M^* \cdot ADP \cdot P_i$ intermediate to actin. From the above discussions, both switch 1 and switch 2 are initially in the closed state (i.e. Mcc·D·P in figure 7). The equilibrium to form the open switch 2 state (i.e. Mco·D·P) appears unfavourable (cf. equation (3.2), step 4), and from thermodynamic balance this equilibrium would also apply to the A·Mcc·D·P $\leftrightarrow$ A·Mco·D·P transition. An alternative actin activation mechanism is required. A feasible mechanism is suggested by structural evidence (Coureux *et al.* 2003; Holmes *et al.* 2003; Reubold *et al.* 2003), and our supporting kinetic studies with the switch 1 mutants W239+ and W242+, which involves actin-induced cleft closure and concomitant opening of switch 1. Furthermore, if switch 1 opens before switch 2 and switch 1 opening is sufficient for release of P_i, then futile cycling is minimized (i.e. routes where switch 2 opening occurs before actin binding). The A·Moc·D state formed initially upon P_i release will spontaneously convert to A·Moo·D with concomitant swinging of the lever arm. The properties of A·MocD would fit the AM'·ADP state of Sleep & Hutton (1980) which was proposed to exist at significant concentrations only during the steady-state ATP turnover, to account for rapid ATP $\leftrightarrow P_i$ exchange. The closed switch 2 state of A·Moc·D may provide a mechanism for stronger P_i binding than that of A·Moo·D, the complex formed by addition of ADP to A·M. However, the open state of switch 1, and hence closed cleft, would result in relatively slow actin dissociation, as required to commit the cross-bridge to force generation. Under load, the lever arm swing will tend to be inhibited, favouring the switch 2 closed states and generating an increased concentration of A·Moc·D, thus accounting for the increased ATP $\leftrightarrow P_i$ exchange under isometric conditions (Sleep & Hutton 1980).

The highlighted route shown in figure 7 is at variance with several physiological studies that have been modelled with the tension generation associated with states before P_i release (Dantzig *et al.* 1992; Ranatunga *et al.* 2002). However, the latter conclusion depends on the details of the models and assumptions about the rate constants for P_i binding and release. It is evident from figure 7 that as $[P_i]$ is increased, A·Moc·D·P will build up, because of the preferential binding of P_i by A·Moc·D, and thus the lever arm swing may occur by the normally minor route via A·Moo·D·P.

The scheme of figure 7 is oversimplified in that there is no explanation for faster release of ADP from the A·Moo·D state (i.e. the state generated by ADP addition to A·Moo) compared with the Moo·D state. It is likely that switch 1 does not operate in a simple two-state open–closed mode. Switch 1 residues interact with both the γ-P_i group as well as the Mg^{2+} ion. Partial movement of switch 1 may be sufficient to release P_i, but further movement might be required to break the bond to Mg^{2+} and thereby allow $Mg \cdot ADP$ release. Early kinetic studies showed that Mg^{2+} and ADP are released together, at least in the absence of actin (Mandelkow & Mandelkow 1973; Bagshaw & Trentham 1974).

Despite its limitations, the mechanism in figure 7 shows how mechano-chemical coupling can be achieved without a direct influence of actin on switch 2 or lever arm position. Rather, actin has an indirect effect via activation of P_i release. However, it has been questioned whether the lever arm swing is the only contribution to the working stroke (Huxley 2000). It is possible that some angular change is associated with the docking of the myosin head on the actin, i.e. the weak to strong transition states associated with the A·Mcc·D·P to A·Moc·D·P transition (Bershitsky *et al.* 1997). More recently, Holmes *et al.* (2004) have suggested a structural model in which the strong binding of actin allows the lever arm to swing without the opening of switch 2. While this model provides another mechanism for avoiding futile cycling, our data with ATPγS lend no support for this idea, as will be discussed elsewhere (Conibear *et al.* 2004).

8. PROBLEMS AND PROSPECTS

The kinetic data obtained from single tryptophan residues can be rationalized in terms of current crystal structures to produce a more detailed working model of the cross-bridge cycle. However it was clear, even from the first few structures produced, that nucleotides with different biochemical properties could induce essentially the same crystal structure, e.g. Dd myosin II apo, Mg·ATP, Mg·AMP·PNP and Mg·ADP all yielded states with a closed switch 1 and open switch 2 (Fisher *et al.* 1995; Gulick *et al.* 1997; Bauer *et al.* 2000). Thus, either the structural differences that determine the kinetics and thermodynamics of nucleotide binding are too small to be discerned by crystallography, and/or these nucleotides produce different distribution of states and crystallization favours one specific state that is common to all. The latter is not necessarily the most abundant state in solution. The sampling by crystallography is most clearly seen in the M·ADP·BeFx state, where solution studies reveal a mixture of switch 2 open and closed conformers in equilibrium on the millisecond time-scale (Malnasi-Csizmadia *et al.* 2001), whereas crystal structures reveal either a

open or closed state depending on the crystallization conditions (Holmes & Geeves 2000).

One aspect of structure–function relationships that requires clarification is the status of the so-called thiol helix in the converter domain. In all Dd structures so far, this appears as an intact helix. However, solution studies on skeletal myosin, which has two reactive thiol groups at each end of the helix, have shown that the thiols can be cross-linked and suggested that the helix may melt during part of the ATPase cycle (Miller *et al.* 1982; Huston *et al.* 1988). Further work suggested that the melted helix, which allowed short cross-linkers to react, might only be a transient species (Kliche *et al.* 1999). Scallop adductor muscle myosin has been crystallized in the presence of ADP with a disordered helix, and appears to decouple the position of the lever from the status of switch 2 (Houdusse *et al.* 2000). Cohen and colleagues (Houdusse *et al.* 2000) argued that this helix melting is essential for the formation of the detached state and thus would be equivalent to $M^{\dagger} \cdot ATP$.

The importance of the thiol helix is illustrated by a rare myosin myopathy that has been identified in a Swedish family. A mutation of E706K in human myosin heavy chain IIa is autosomal dominant and leads to muscle weakness, joint contractures and ophthalmoplegia (Martinsson *et al.* 2000; Tajsharghi *et al.* 2002). The thiol helix is conserved throughout the myosin II family (CNGVLEGIR-IcR), although the second cysteine (lower case c), equivalent of reactive thiol SH1 of vertebrate myosin, is not conserved (the equivalent Dd residue is T). The glutamate residue (shown in bold) is, however, strongly conserved. We have recently constructed the equivalent mutation in Dd (E683K) in a W501+ background to probe the effects of this substitution.

The basal steady-state ATPase of E683K is close to that of W501+, but actin activation is reduced by an order of magnitude, as is the K_m for actin. The fluorescence from W501 in the E683K mutant is slightly reduced in amplitude and notably ADP binding no longer caused a quench in fluorescence. With ATP, the maximum rate of the fluorescence enhancement is reduced to 8 s^{-1}, suggesting that the coupled open–closed and hydrolysis step is reduced about threefold. ATP dissociates acto-E683K, but the reaction is slowed by an order of magnitude compared with W501 and wild-type motor domain. These effects would lead to a higher duty ratio in the cycle and a reduced velocity of contraction. Such a 'braking' action would account for the dominance of this mutation in muscle tissue. Interestingly, the diseased state is progressive and only becomes severe as the level of the myosin IIa isoform rises with age (Tajsharghi *et al.* 2002). E683 is a surface residue and might not appear critical for folding or actomyosin interactions. However, in the thiol helix, a conserved arginine residue is located three residues away and thus these side chains would be close in space. Mutation to E683K would result in charge repulsion instead of attraction, leading to a kinked and/or more unstable helix. This might account for the reduced W501 fluorescence change because the converter domain could not go through its full range of movement about the relay loop. Mutations of the conserved glycine residues in the thiol helix have also proven detrimental (Batra *et al.* 1999).

In summary, it can be seen that fluorescence probes can be introduced into defined parts of the myosin molecule

and that this approach allows a more rigorous analysis of the kinetic pathway. The crystal structures of myosin have allowed a rational approach to the introduction of probe molecules. In turn, the kinetic data have helped to order the sequence of events and identify states that have precluded crystallization.

REFERENCES

Bagshaw, C. R. & Trentham, D. R. 1973 The reversibility of adenosine triphosphate cleavage by myosin. *Biochem. J.* **133**, 323–328.

Bagshaw, C. R. & Trentham, D. R. 1974 The characterization of myosin-product complexes and of product-release steps during the magnesium ion-dependent adenosine triphosphatase reaction. *Biochem. J.* **141**, 331–349.

Bagshaw, C. R., Eccleston, J. F., Trentham, D. R., Yates, D. W. & Goody, R. S. 1972 Transient kinetic studies of the Mg^{2+}-dependent ATPase of myosin and its proteolytic subfragments. *Cold Spring Harbor Symp. Quant. Biol.* **37**, 127–135.

Bagshaw, C. R., Eccleston, J. F., Eckstein, F., Goody, R. S., Gutfreund, H. & Trentham, D. R. 1974 The magnesium ion-dependent adenosine triphosphatase of myosin. Two-step processes of adenosine triphosphate association and adenosine diphosphate dissociation. *Biochem. J.* **141**, 351–364.

Bagshaw, C. R., Trentham, D. R., Wolcott, R. G. & Boyer, P. D. 1975 Oxygen exchange in the g-phosphoryl group of protein-bound ATP during Mg^{2+}-dependent adenosine triphosphatase activity of myosin. *Proc. Natl Acad. Sci. USA* **72**, 2592–2596.

Batra, R. & Manstein, D. J. 1999 Functional characterisation of *Dictyostelium* myosin II with conserved tryptophanyl residue 501 mutated to tyrosine. *Biol. Chem.* **380**, 1017–1023.

Batra, R., Geeves, M. A. & Manstein, D. J. 1999 Kinetic analysis of *Dictyostelium discoideum* myosin motor domains with glycine-to-alanine mutations in the reactive thiol region. *Biochemistry* **38**, 6126–6134.

Bauer, C. B., Holden, H. M., Thoden, J. B., Smith, R. & Rayment, I. 2000 X-ray structures of the apo and MgATP-bound states of *Dictyostelium discoideum* myosin motor domain. *J. Biol. Chem.* **275**, 38 494–38 499.

Bershitsky, S. Y., Tsaturyan, A. K., Bershitskaya, O. N., Mashanov, G. I., Brown, P., Burns, R. & Ferenczi, M. A. 1997 Muscle force is generated by myosin heads stereospecifically attached to actin. *Nature* **388**, 186–190.

Conibear, P. B., Bagshaw, C. R., Fajer, P. G., Kovacs, M. & Malnasi-Csizmadia, A. 2003 Myosin cleft movement and its coupling to actomyosin dissociation. *Nature Struct. Biol.* **10**, 831–835.

Conibear, P. B., Malnasi-Csizmadia, A. & Bagshaw, C. R. 2004 The effect of F-actin on the relay helix position of myosin II, as revealed by tryptophan fluorescence, and its implications for mechanochemical coupling. *Biochemistry*. (In the press.)

Coureux, P. D., Wells, A. L., Menetrey, J., Yengo, C. M., Morris, C. A., Sweeney, H. L. & Houdusse, A. 2003 A structural state of the myosin V motor without bound nucleotide. *Nature* **425**, 419–423.

Dantzig, J. A., Goldman, Y. E., Millar, N. C., Lacktis, J. & Homsher, E. 1992 Reversal of the cross-bridge force-generating transition by photogeneration of phosphate in rabbit psoas muscle fibres. *J. Physiol.* **451**, 247–278.

Fisher, A. J., Smith, C. A., Thoden, J. B., Smith, R., Sutoh, K., Holden, H. M. & Rayment, I. 1995 X-ray structures of the myosin motor domain of *Dictyostelium discoideum* complexed with MgADP.BeF$_x$ and MgADP.AlF$_4$. *Biochemistry* **34**, 8960–8972.

Geeves, M. A. & Holmes, K. C. 1999 Structural mechanism of muscle contraction. *A. Rev. Biochem.* **68**, 687–728.

Goody, R. S., Hofmann, W. & Mannherz, G. H. 1977 The binding constant of ATP to myosin S1 fragment. *Eur. J. Biochem.* **78**, 317–324.

Gulick, A. M., Bauer, C. B., Thoden, J. B. & Rayment, I. 1997 X-ray structures of the MgADP, MgATPgS and MgAMPPNP complexes of the *Dictyostelium discoideum* myosin motor domain. *Biochemistry* **36**, 11 619–11 628.

Holmes, K. C. & Geeves, M. A. 2000 The structural basis of muscle contraction. *Phil. Trans. R. Soc. B* **355**, 419–431. (doi:10.1098/rstb.2000.0583)

Holmes, K. C., Angert, I., Kull, F. J., Jahn, W. & Schroder, R. R. 2003 Electron cryo-microscopy shows how strong binding of myosin to actin releases nucleotide. *Nature* **425**, 423–427.

Holmes, K. C., Schröder, R. R. , Eschenburg, S., Sweeney, H. L. & Houdusse, A. 2004 The structure of the rigor complex and its implications for the power stroke. *Phil. Trans. R. Soc. B* **359**, 1819–1828. (doi:10.1098/rstb.2004.1566)

Houdusse, A., Szent-Gyorgyi, A. G. & Cohen, C. 2000 Three conformational states of scallop myosin S1. *Proc. Natl Acad. Sci. USA* **97**, 11238–11243.

Huston, E. E., Grammer, J. C. & Yount, R. G. 1988 Flexibility of the myosin heavy chain: direct evidence that the region containing SH1 and SH2 can move 10 Å under the influence of nucleotide binding. *Biochemistry* **27**, 8945–8952.

Huxley, A. F. 1957 Muscle structure and theories of contraction. *Prog. Biophys. Biophys. Chem.* 7, 255–318.

Huxley, A. F. & Niedergerke, R. 1954 Structural changes in muscle during contraction. *Nature* **173**, 971–973.

Huxley, H. E. 1969 The mechanism of muscular contraction. *Science* **164**, 1356–1365.

Huxley, H. E. 2000 Past, present and future experiments on muscle. *Phil. Trans. R. Soc. B* **355**, 539–543. (doi:10.1098/rstb.2000.0595)

Huxley, H. E. & Hanson, J. 1954 Changes in the cross-striations of muscle during contraction and stretch and their structural interpretation. *Nature* **173**, 973–976.

Johnson, K. A. & Taylor, E. W. 1978 Intermediate states of subfragment 1 and actosubfragment 1 ATPase: reevaluation of the mechanism. *Biochemistry* **17**, 3432–3442.

Kliche, W., Pfannstiel, J., Tiepold, M., Stoeva, S. & Faulstich, H. 1999 Thiol-specific cross-linkers of variable length reveal a similar separation of SH1 and SH2 in myosin subfragment 1 in the presence and absence of MgADP. *Biochemistry* **38**, 10 307–10 317.

Kovacs, M., Malnasi-Csizmadia, A., Woolley, R. J. & Bagshaw, C. R. 2002 Analysis of nucleotide binding to *Dictyostelium* myosin II motor domains containing a single tryptophan near the active site. *J. Biol. Chem.* **277**, 28459–28467.

Kuhlman, P. A. & Bagshaw, C. R. 1998 ATPase kinetics of the *Dictyostelium discoideum* myosin II motor domain. *J. Muscle Res. Cell Motil.* **19**, 491–504.

Kurzawa, S. E., Manstein, D. J. & Geeves, M. A. 1997 Dictyostelium discoideum myosin II: characterization of functional myosin motor fragments. *Biochemistry* **36**, 317–323.

Lehrer, S. S. 1997 Intramolecular pyrene excimer fluorescence: a probe of proximity and protein conformational change. *Meth. Enzymol.* **278**, 286–295.

Lymn, R. W. & Taylor, E. W. 1971 Mechanism of adenosine triphosphate hydrolysis by actomyosin. *Biochemistry* **10**, 4617–4624.

Malnasi-Csizmadia, A., Woolley, R. J. & Bagshaw, C. R. 2000 Resolution of conformational states of *Dictyostelium* myosin II motor domain using tryptophan (W501) mutants: implications for the open-closed transition identified by crystallography. *Biochemistry* **39**, 16135–16146.

Malnasi-Csizmadia, A., Pearson, D. S., Kovacs, M., Woolley, R. J., Geeves, M. A. & Bagshaw, C. R. 2001 Kinetic resolution of a conformational transition and the ATP hydrolysis step using relaxation methods with a *Dictyostelium* myosin II mutant containing a single tryptophan residue. *Biochemistry* **40**, 12 727–12 737.

Mandelkow, E. M. & Mandelkow, E. 1973 Fluorimetric studies on the influence of metal ions and chelators on the interaction between myosin and ATP. *FEBS Lett.* **33**, 161–166.

Mannherz, H. G., Schenck, H. & Goody, R. S. 1974 Synthesis of ATP from ADP and inorganic phosphate at the myosin-subfragment 1 active site. *Eur. J. Biochem.* **48**, 287–295.

Martinsson, T., Oldfors, A., Darin, N., Berg, K., Tajsharghi, H., Kyllerman, M. & Wahlstrom, J. 2000 Autosomal dominant myopathy: missense mutation (Glu-706 → Lys) in the myosin heavy chain IIa gene. *Proc. Natl Acad. Sci. USA* **97**, 14 614–14 619.

Millar, N. C. & Geeves, M. A. 1988 Protein fluorescence changes associated with ATP and adenosine 5'-[γ-thio]-triphosphate binding to skeletal muscle myosin subfragment 1 and actomyosin subfragment 1. *Biochem. J.* **249**, 735–743.

Miller, L., Coppedge, J. & Reisler, E. 1982 The reactive SH1 and SH2 cysteines in myosin subfragment 1 are cross-linked at similar rates with reagents of different length. *Biochem. Biophys. Res. Commun.* **106**, 117–122.

Onishi, H., Konishi, K., Fujiwara, K., Hayakawa, K., Tanokura, M., Martinez, H. M. & Morales, M. F. 2000 On the tryptophan residue of smooth muscle myosin that responds to binding of nucleotide. *Proc. Natl Acad. Sci. USA* **97**, 11 203–11 208.

Park, S. & Burghardt, T. P. 2000 Isolating and localizing ATP-sensitive tryptophan emission in skeletal myosin subfragment 1. *Biochemistry* **39**, 11 732–11 741.

Ranatunga, K. W., Coupland, M. E. & Mutungi, G. 2002 An asymmetry in the phosphate dependence of tension transients induced by length perturbation in mammalian (rabbit psoas) muscle fibres. *J. Physiol.* **542**, 899–910.

Rayment, I., Holden, H. M., Whittaker, M., Yohn, C. B., Lorenz, M., Holmes, K. C. & Milligan, R. A. 1993*a* Structure of the actin–myosin complex and its implications for muscle contraction. *Science* **261**, 58–65.

Rayment, I., Rypniewski, W. R., Schmidt-Base, K., Smith, R., Tomchick, D. R., Benning, M. M., Winkelmann, D. A., Wesenberg, G. & Holden, H. M. 1993*b* Three-dimensional structure of myosin subfragment-1: a molecular motor. *Science* **261**, 50–58.

Reubold, T. F., Eschenburg, S., Becker, A., Kull, F. J. & Manstein, D. J. 2003 A structural model for actin-induced nucleotide release in myosin. *Nature Struct. Biol.* **10**, 826–830.

Ritchie, M. D., Geeves, M. A., Woodward, S. K. & Manstein, D. J. 1993 Kinetic characterization of a cytoplasmic myosin motor domain expressed in *Dictyostelium discoideum*. *Proc. Natl Acad. Sci. USA* **90**, 8619–8623.

Ruppel, K. M. & Spudich, J. A. 1996 Structure-function analysis of the motor domain of myosin. *A. Rev. Cell Dev. Biol.* **12**, 543–573.

Sasaki, N., Shimada, T. & Sutoh, K. 1998 Mutational analysis of the switch II loop of *Dictyostelium* myosin II. *J. Biol. Chem.* **273**, 20 334–20 340.

Sasaki, N., Ohkura, R. & Sutoh, K. 2003 *Dictyostelium* myosin II mutations that uncouple the converter swing and ATP hydrolysis cycle. *Biochemistry* **42**, 90–95.

Shih, W. M., Gryczynski, Z., Lakowicz, J. R. & Spudich, J. A. 2000 A FRET-based sensor reveals large ATP hydrolysis-induced conformational changes and three distinct states of the molecular motor myosin. *Cell* **102**, 683–694.

Shimada, T., Sasaki, N., Ohkura, R. & Sutoh, K. 1997 Alanine scanning mutagenesis of the switch I region in the ATPase site of *Dictyostelium discoideum* myosin II. *Biochemistry* **36**, 14 037–14 043.

Sleep, J. A. & Hutton, R. L. 1980 Exchange between inorganic phosphate and adenosine 5'-triphosphate in the medium by actomyosin subfragment 1. *Biochemistry* **19**, 1276–1283.

Smith, C. A. & Rayment, I. 1996 X-ray structure of the magnesium(II).ADP.vanadate complex of the *Dictyostelium discoideum* myosin motor domain to 1.9 Å resolution. *Biochemistry* **35**, 5404–5417.

Steffen, W. & Sleep, J. 2004 Using optical tweezers to relate the chemical and mechanical cross-bridge cycles. *Phil. Trans. R. Soc. B* **359**, 1857–1865. (doi:10.1098/rstb.2004. 1558)

Steffen, W., Smith, D. & Sleep, J. 2003 The working stroke upon myosin-nucleotide complexes binding to actin. *Proc. Natl Acad. Sci. USA* **100**, 6434–6439.

Suzuki, Y., Yasunaga, T., Ohkura, R., Wakabayashi, T. & Sutoh, K. 1998 Swing of the lever arm of a myosin motor at the isomerization and phosphate-release steps. *Nature* **396**, 380–383.

Tajsharghi, H., Thornell, L. E., Darin, N., Martinsson, T., Kyllerman, M., Wahlstrom, J. & Oldfors, A. 2002 Myosin heavy chain IIa gene mutation E706K is pathogenic and its expression increases with age. *Neurology* **58**, 780–786.

Taylor, E. W. 1977 Transient phase of adenosine triphosphate hydrolysis by myosin, heavy meromyosin, and subfragment 1. *Biochemistry* **16**, 732–739.

Trybus, K. M. & Taylor, E. W. 1982 Transient kinetics of adenosine 5'-diphosphate and adenosine 5'-(β, γ-imidotriphosphate) binding to subfragment 1 and actosubfragment 1. *Biochemistry* **21**, 1284–1294.

Urbanke, C. & Wray, J. 2001 A fluorescence temperature-jump study of conformational transitions in myosin subfragment 1. *Biochem. J.* **358**, 165–173.

Wachter, R. M. & Remington, S. J. 1999 Sensitivity of the yellow variant of green fluorescent protein to halides and nitrate. *Curr. Biol.* **9**, R628–629.

Wakelin, S. & Bagshaw, C. R. 2003 A prism combination for near isotropic fluorescence excitation by total internal reflection. *J. Microsc.* **209**, 143–148.

Wakelin, S., Conibear, P. B., Woolley, R. J., Floyd, D. N., Bagshaw, C. R., Kovacs, M. & Malnasi-Csizmadia, A. 2002 Engineering *Dictyostelium discoideum* myosin II for the introduction of site-specific probes. *J. Muscle Res. Cell Motil.* **24**, 673–683.

Xiao, M., Reifenberger, J. G., Wells, A. L., Baldacchino, C., Chen, L. Q., Ge, P., Sweeney, H. L. & Selvin, P. R. 2003 An actin-dependent conformational change in myosin. *Nature Struct. Biol.* **10**, 402–408.

Yengo, C. M., Chrin, L. R., Rovner, A. S. & Berger, C. L. 2000 Tryptophan 512 is sensitive to conformational changes in the rigid relay loop of smooth muscle myosin during the MgATPase cycle. *J. Biol. Chem.* **275**, 25481–25487.

Yount, R. G., Lawson, D. & Rayment, I. 1995 Is myosin a 'back door' enzyme? *Biophys. J.* **68**, 44S–47S.

GLOSSARY

A: actin

ADP: adenosine 5'- diphosphate

AMP·PNP: adenosine 5'-(β,γ-imidotriphosphate)

AMPγS: adenosine 5'-*O*-(3-thiotriphosphate)

ATP: adenosine 5' triphosphate

BeFx: beryllium fluoride with undefined stoichiometry

BFP: blue fluorescent protein

CFP: cyan fluorescent protein

Dd: *Dictyostelium discoideum*

FRET: fluorescence resonance energy transfer

GFP: green fluorescent protein

HEPES: N-(2-hydroxyethyl)piperazine-N'(2-ethane-suphonic acid)

M: myosin motor domain

pdb: protein database file (with accession code)

P_i: phosphate

V_i: vanadate

YFP: yellow fluorescent protein